Supporting Information

Effective Antiscaling Performance of Reverse-Osmosis Membranes Made of Carbon Nanotubes and Polyamide Nanocomposites

Yoshihiro Takizawa,[a] Shigeki Inukai,[a] Takumi Araki,[a,c] Rodolfo Cruz-Silva,[a,b,*] Josue Ortiz-Medina,[a] Aaron Morelos-Gomez,[a] Syogo Tejima,[a,c] Ayaka Yamanaka,[a,c] Michiko Obata,[b] Auppatham Nakaruk,[a] Kenji Takeuchi,[a,b] Takuya Hayashi,[a,b] Mauricio Terrones,[b,d] and Morinobu Endo[a,b,*]

[a] Global Aqua Innovation Center, and [b] Institute of Carbon Science and Technology, Shinshu University; 4-17-1 Wakasato, Nagano 380-8553, Japan.

[c] Research Organization for Information Science & Technology; 2-32-3, Kitashinagawa, Shinagawa-ku, Tokyo 140-0001.

[d] Department of Physics, Department of Materials Science and Engineering, and Department of Chemistry. The Pennsylvania State University; University Park, Pennsylvania 16802, USA.

*Corresponding author's email addresses:

rcruzsilva@shinshu-u.ac.jp

endo@endomoribu.shinshu-u.ac.jp

Index

S1. Supporting information on experimental methods

Supporting Figures

S1. Supporting information on experimental methods

S1.1. $CaCO_3$ Nucleation in static conditions

MWCNT-PA and plain PA membranes were synthesized in liquid/liquid interfacial polymerization and transferred to silicon wafers. The membranes were immersed in a freshly prepared mixture $CaCl_2$ (1.0 mol/L) and $NaHCO_3$ (1.0 mol/L) aqueous solutions at room temperature for 1 min. The membranes were then removed, washed with distilled water and dried.

S1.2. Salt rejection and permeate flux measurements

The NaCl rejection, R (%), was calculated using the following Equation (1S)

$$R = \frac{C_f - C_p}{C_f} \times 100\ (\%) \tag{1S}$$

where C_f and C_p are the feed and the permeate concentrations of the solution, respectively. The values of C_f and C_p were obtained from the electrical conductivity measurement of the solutions by using an electrical conductivity meter (ES-71, Horiba, Kyoto, Japan) with suitable conducting electrodes (9382-10D and 3574-10C, Horiba) for source water and permeate water, respectively.

The permeate flux, J ($Lm^{-2}h^{-1}$), was calculated using Equation (2S)

$$J = \frac{\Delta V}{A\Delta t}\ (\mathrm{L}m^{-2}h^{-1}) \tag{2S}$$

where ΔV (L) is the volume of permeated water collected during the permeation time Δt (h) and A (m^2) is the effective surface area of the membrane samples.

The normalized permeate flux $J_r(t)$ was calculated using Equation (3S):

$$J_r(t) = J(t)/J_0 \tag{3S}$$

where $J(t)$ is the flux after the addition of BSA and J_o is the flux after the compaction of the membrane.

S1.3. Molecular dynamics simulation details

During the simulations, we used the SPC/Fw model for the water molecules[1-2] and the General Amber Force Field (GAFF)[3] to simulate the G-PA and plain PA. The plain PA was generally described by GAFF[4-6] and the atom charges for the plain PA were as described by Harder et al.[4] A new set of

charges for G-PA, considering the charge transfer from graphene to PA were calculated using ab initio calculations. The interactions among molecules were calculated using the Lenard-Jones (LJ) model with Lorentz-Berthelot combination rules and Coulomb interactions with particle-particle particle-mesh solver.[7] All MD simulation time steps were set to 1.0 fs and the trajectory data were saved at every 10,000-step interval for the analysis. For the scaling simulation, we set 50 $CaCO_3$ molecules and 19,401 and 15,792 water molecules for the G-PA and plain PA model, respectively. For the $CaCO_3$ scaling, the relaxation was performed for the membrane models and the water system for 2 ns.

Supporting Figures

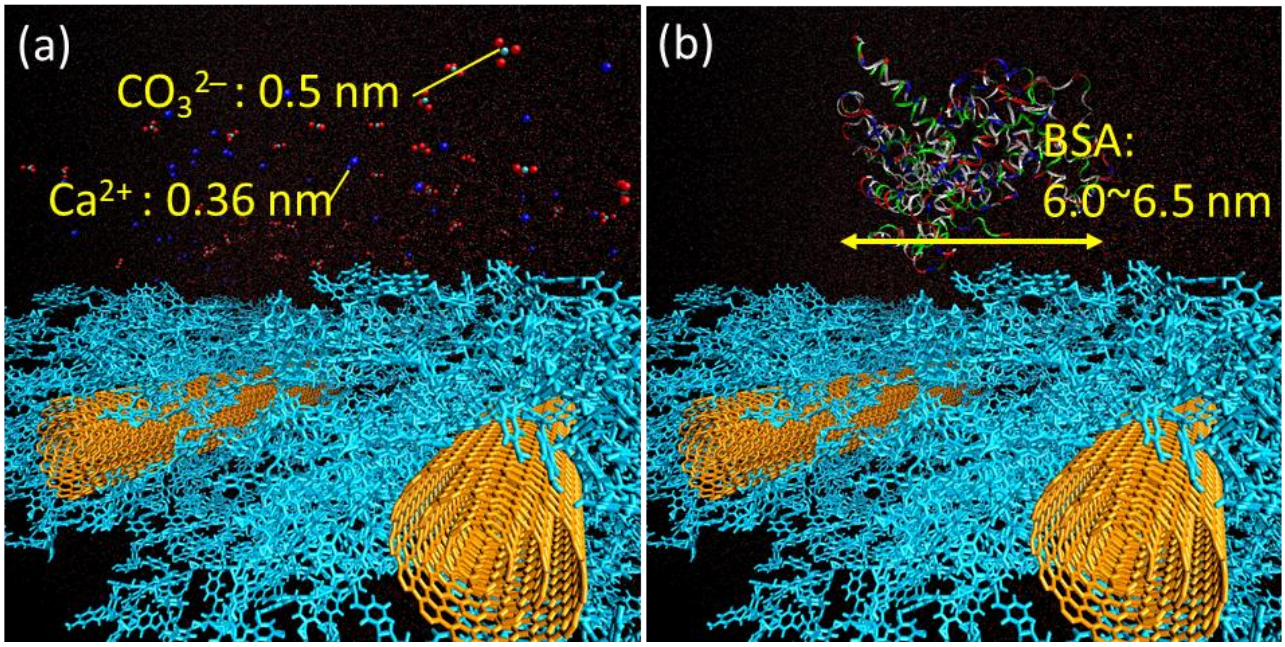

Figure S-1. Computer generated models of the surface of the MWCNT-PA membrane, accompanied by organic and inorganic foulants. Note the difference in size between (**a**) Ca^{2+} and CO_3^{2-} ions and (**b**) bovine serum albumin (BSA) on MWCNT-PA membrane.

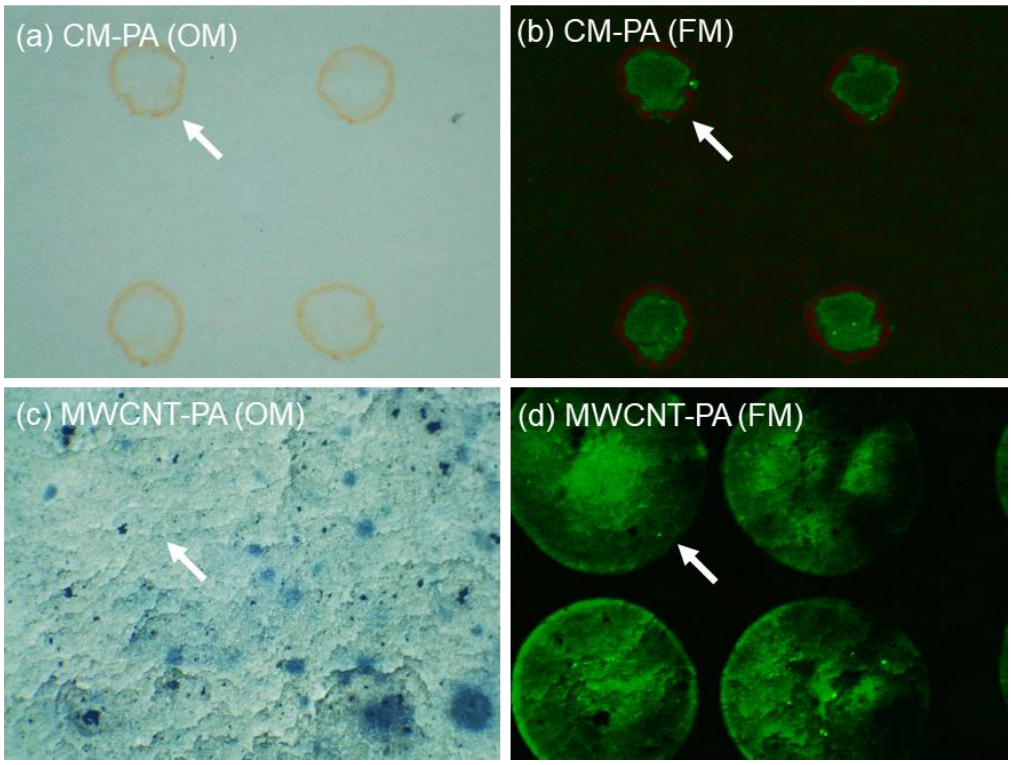

Figure S-2. Fluorescent patterns by droplets of calcein solution observed using optical microscope (OM) and fluorescence microscope (FM) on (**a,b**) CM-PA and (**c,d**) MWCNT-PA membrane. Fluorescence on MWCNT-PA membrane was recognized despite MWCNT is known as a quencher. The diameter of fluorescent patterns made on the membrane became larger on MWCNT-PA membrane, even though the amount of applied fluorescence was same for CM-PA. This could be due to the higher hydrophilicity of MWCNT-PA membrane.[8] The yellow ring patterns seen in the CM-PA (a) show red fluorescence in (b) and are most likely the protective sizing of the membrane.

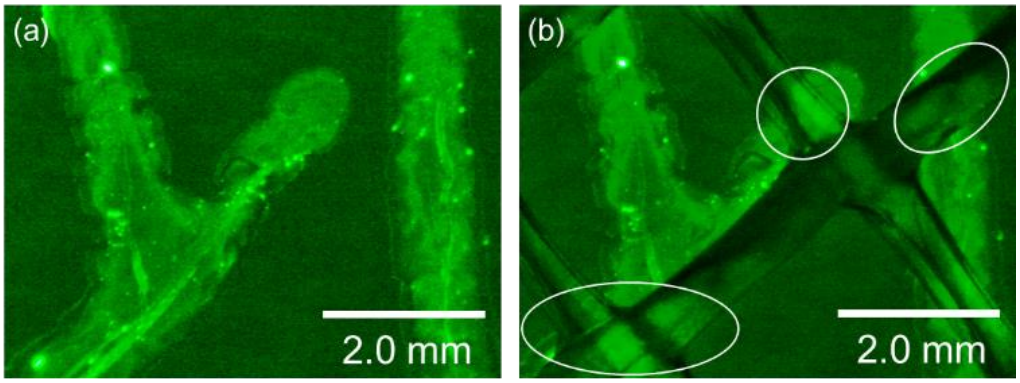

Figure S-3. Fluorescence microscopy images after calcein dying of (**a**) scale on the membrane surface and (**b**) the same scale pattern seen through the spacer. The area circled show the scale seen through the spacer.

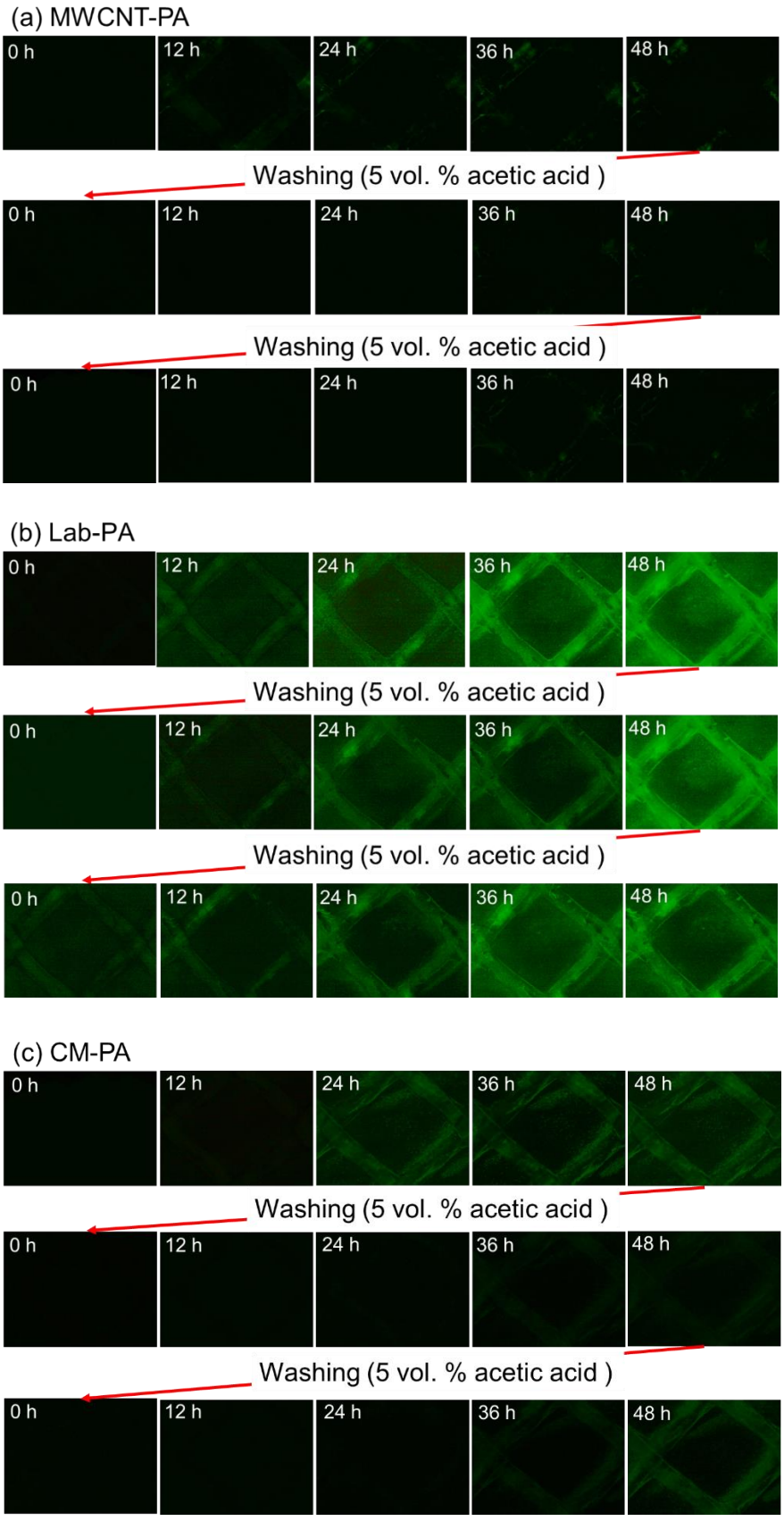

Figure S-4. Fluorescence microscopy images showing three cycles of 48 h of scale deposition including two acid washing steps with diluted acetic acid (**a**) MWCNT-PA, (**b**) lab-PA, and (**c**) CM-PA.

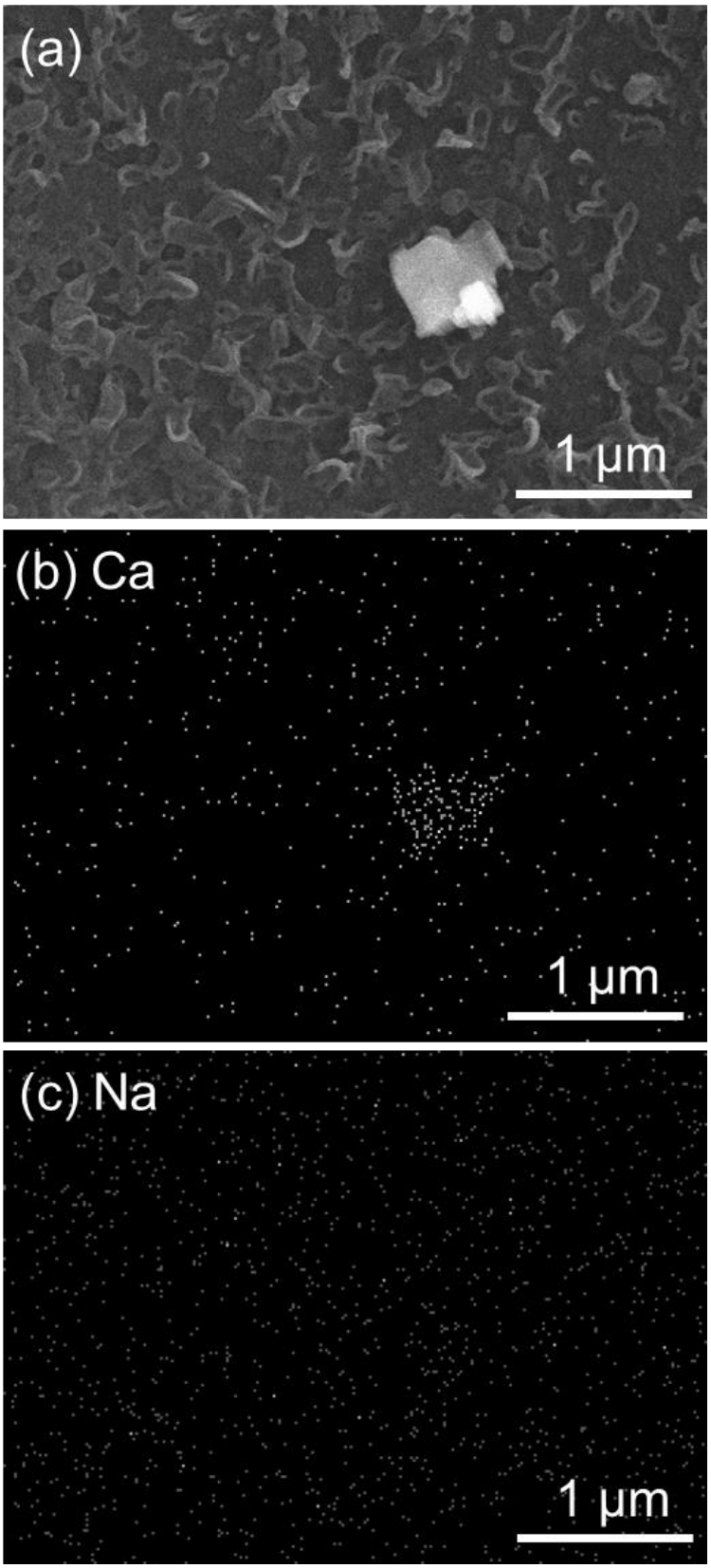

Figure S-5. (**a**) SEM image of $CaCO_3$ scaling on MWCNT-PA membrane and EDX mapping image of (**b**) Ca and (**c**) Na at same field observation.

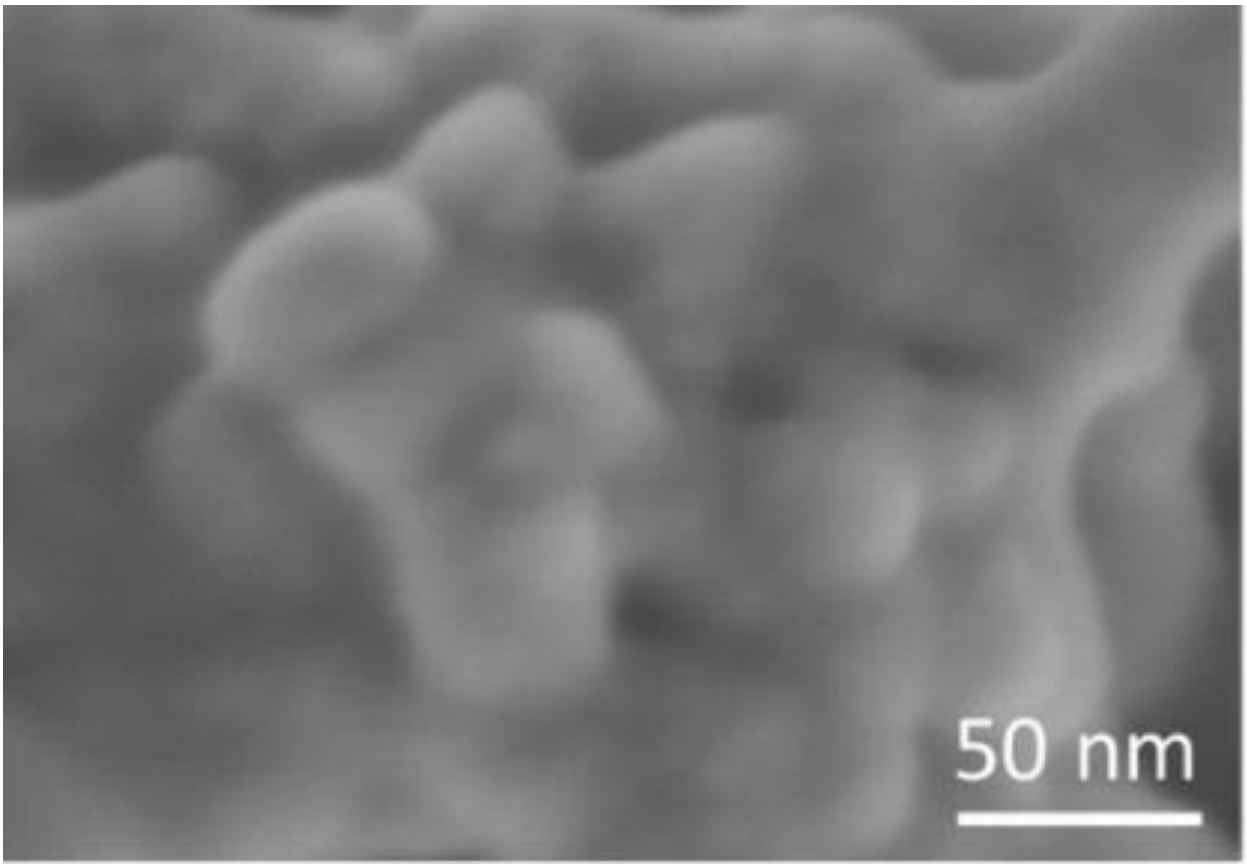

Figure S-6. SEM image of a typical ACC of aggregated particulate, formed on lab-PA membrane and CM-PA.

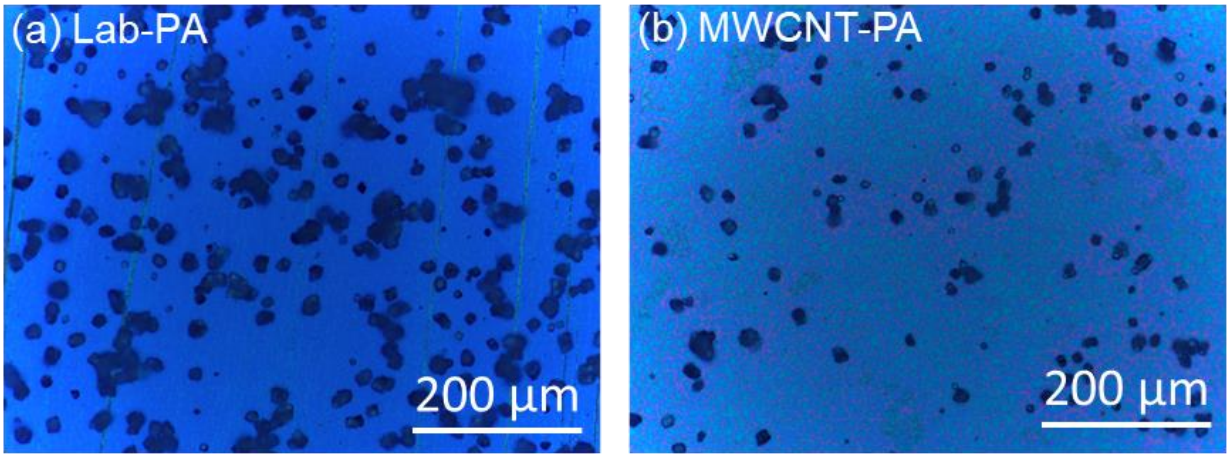

Figure S-7. Optical microscopic images of $CaCO_3$ crystals formed under static conditions on (**a**) the lab-PA membrane and (**b**) MWCNT-PA membrane by quickly mixing 1.0 mol/L-$CaCl_2$ solution and 1.0 mol/L-$NaHCO_3$ solution for 1 min.

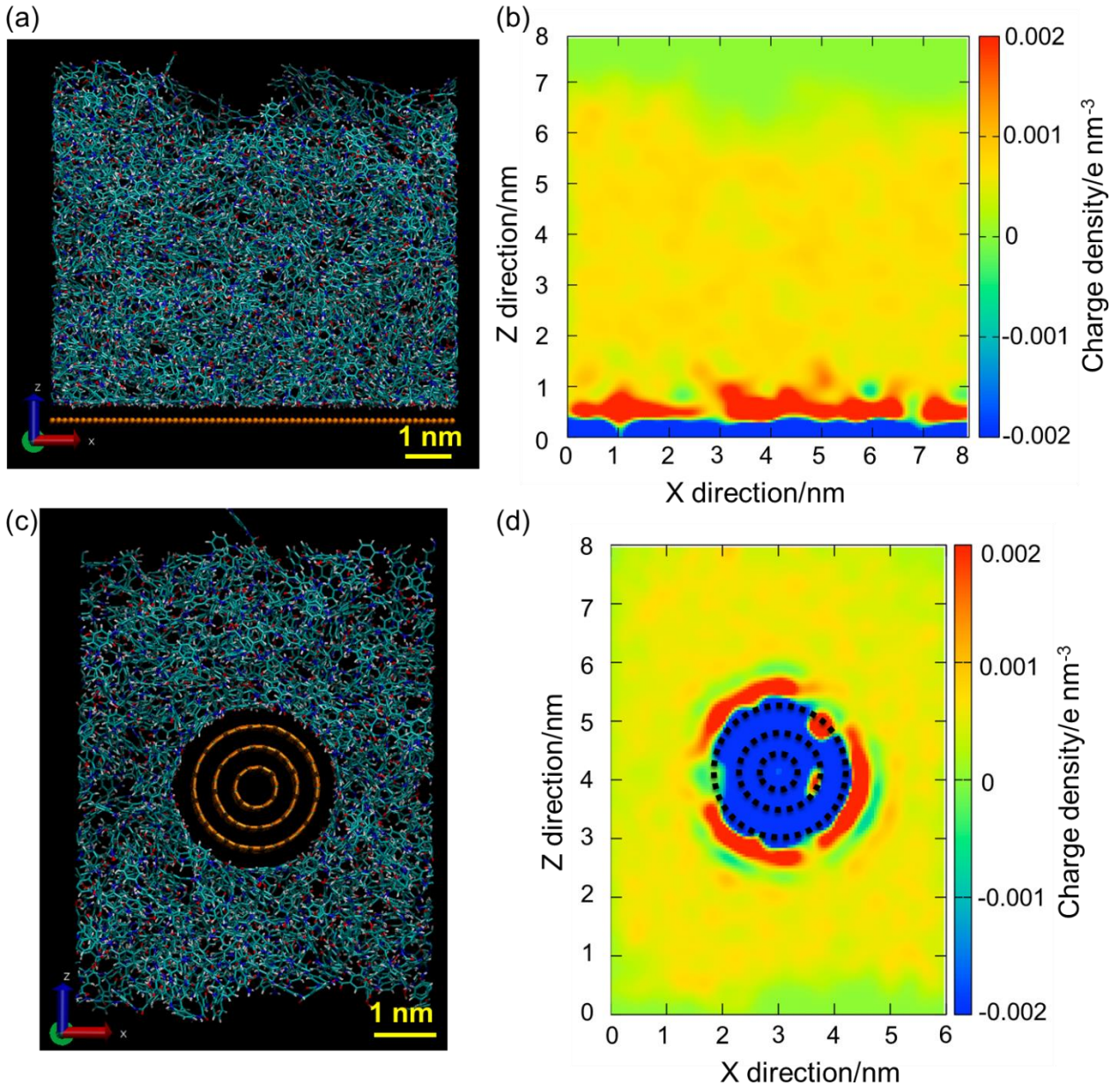

Figure S-8. Three-dimensional model of the (**a**) graphene-polyamide (G-PA) structure. (**b**) Charge transfer density map of G-PA. Three-dimensional model of the (**c**) MWCNT-polyamide structure. (**d**) Charge transfer density map of MWCNT-polyamide. The blue, red, and cyan atoms represent nitrogen, oxygen, and carbon, respectively in Figure S-9a and S-9c. The orange atoms in Figure S-9a and Figure S-9c are the side view of the graphene sheet and MWCNT, respectively.

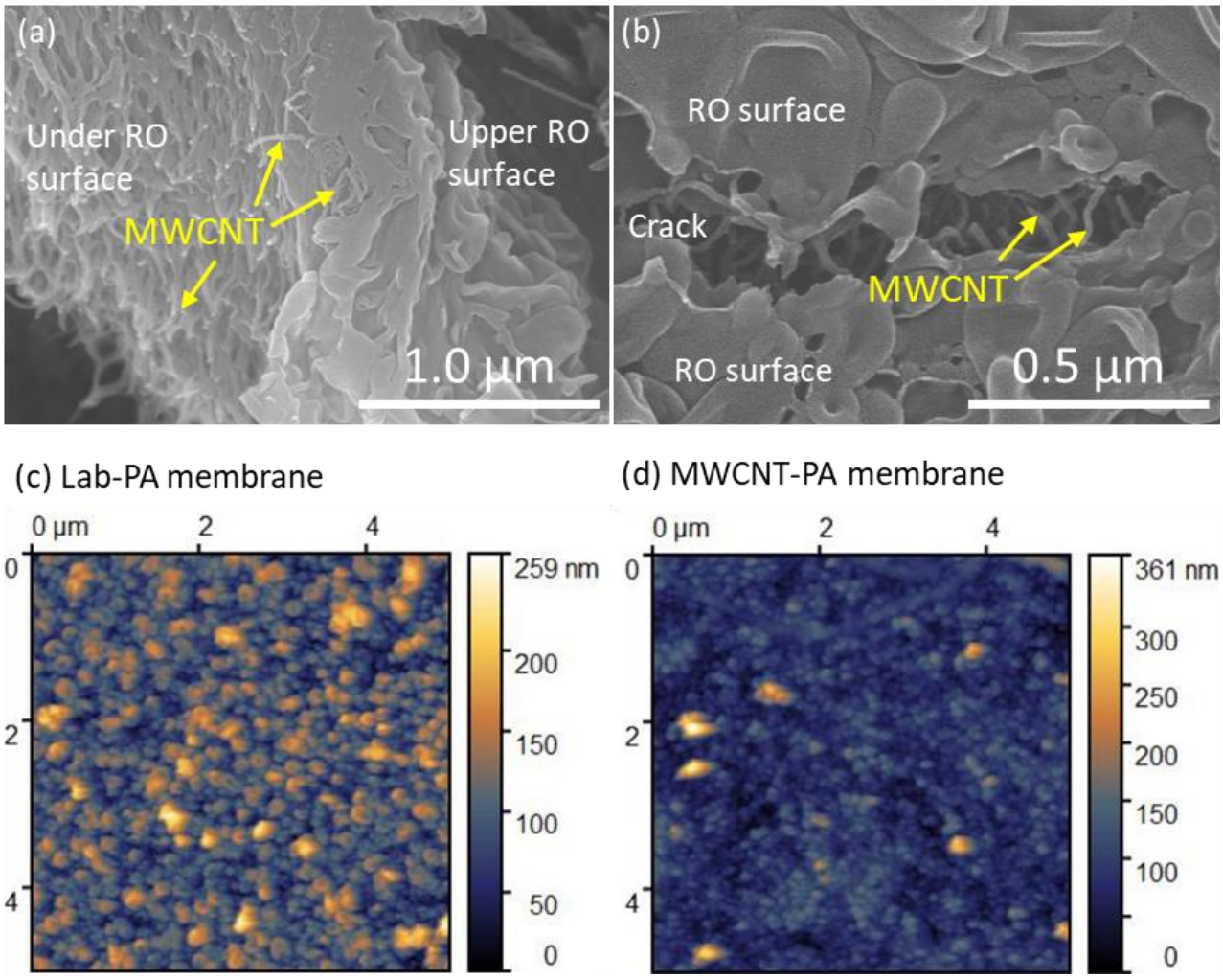

Figure S-9. SEM images showing the MWCNT exposed in the (**a**) peeled-off RO active layer and (**b**) through an induced crack in the RO active layer, AFM height images of (**c**) lab-PA and the (**d**) MWCNT-PA membrane.

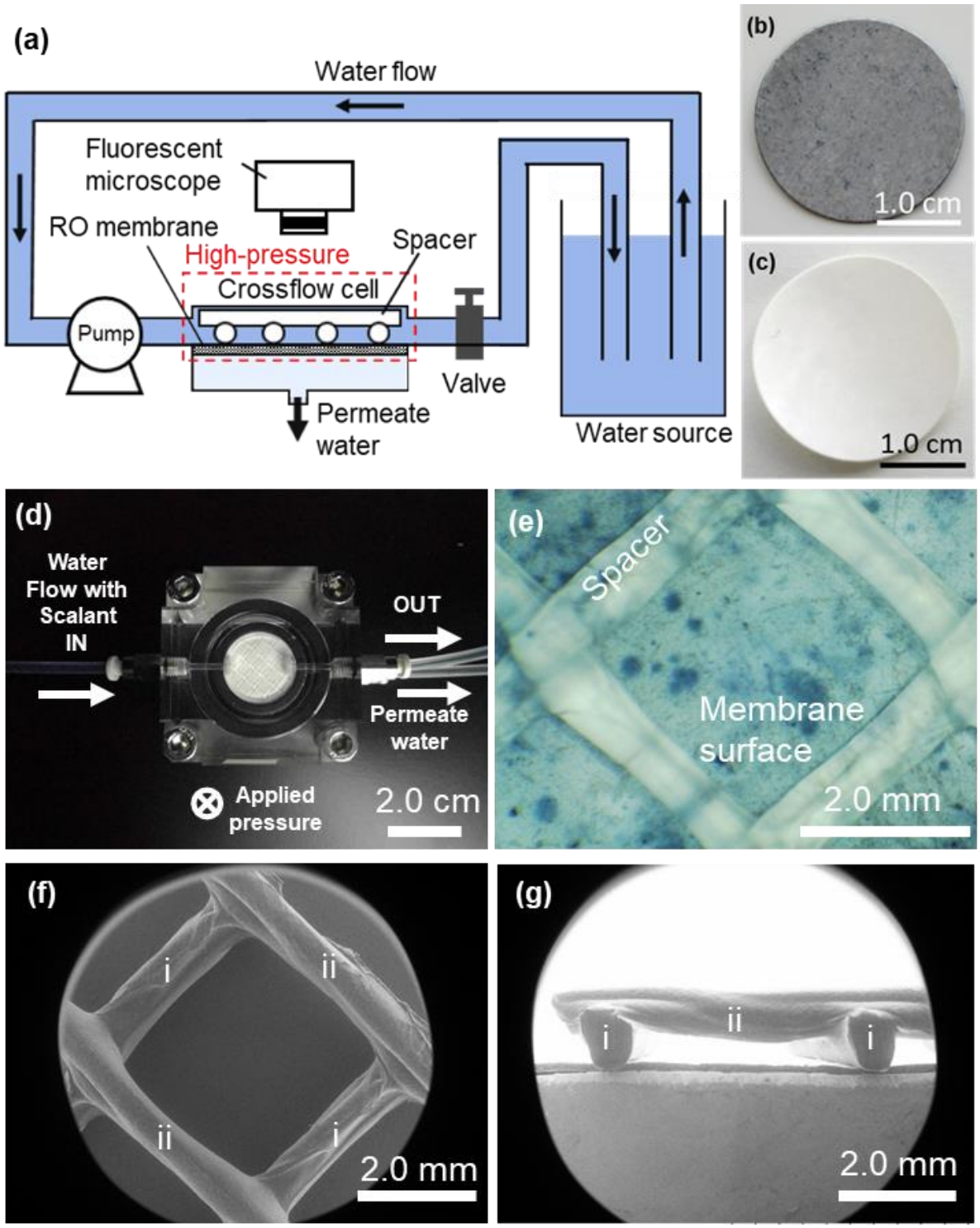

Figure S-10. (**a**) Schematic illustration of the crossflow setup used for the evaluation of the membrane scaling study. Top view of (**b**) the MWCNT-PA membrane and (**c**) the lab-PA membrane. (**d**) Crossflow acrylic cell used during the observation with the fluorescent microscope. (**e**) White light image of the mesh-like spacer on top of the MWCNT-PA membrane surface. SEM images of (**f**) top view and (**g**) side view of the mesh-like spacer (corresponding threads were labeled with i and ii in (**f**) and (**g**)).

References

(1) Raiteri, P.; Gale, J. D., Water Is the Key to Nonclassical Nucleation of Amorphous Calcium Carbonate. *J. Am. Chem. Soc.* **2010,** *132* (49), 17623-17634.

(2) Wu, Y.; Chen, H.; Wang, F.; Paesani, F.; Voth, G. A., An Improved Multistate Empirical Valence Bond Model for Aqueous Proton Solvation and Transport. *J. Phys. Chem. B* **2008,** *112* (2), 467-482.

(3) Cornell, W. D.; Cieplak, P.; Bayly, C. I.; Gould, I. R.; Merz, K. M.; Ferguson, D. M.; Spellmeyer, D. C.; Fox, T.; Caldwell, J. W.; Kollman, P. A., A Second Generation Force Field for the Simulation of Proteins, Nucleic Acids, and Organic Molecules *J. Am. Chem. Soc.* **1995**, 117(19), 5179−5197.

(4) Harder, E.; Walters, D. E.; Bodnar, Y. D.; Faibish, R. S.; Roux, B., Molecular Dynamics Study of a Polymeric Reverse Osmosis Membrane. *J. Phys. Chem. B* **2009,** *113* (30), 10177-10182.

(5) Ding, M.; Szymczyk, A.; Ghoufi, A., On the structure and rejection of ions by a polyamide membrane in pressure-driven molecular dynamics simulations. *Desalination* **2015,** *368*, 76-80.

(6) Shen, M.; Keten, S.; Lueptow, R. M., Dynamics of water and solute transport in polymeric reverse osmosis membranes via molecular dynamics simulations. *J.Membr. Sci.* **2016,** *506*, 95-108.

(7) Pollock, E. L.; Glosli, J., Comments on P3M, FMM, and the Ewald method for large periodic Coulombic systems. *Comput. Phys. Commun.* **1996,** *95* (2), 93-110.

(8) Inukai, S.; Cruz-Silva, R.; Ortiz-Medina, J.; Morelos-Gomez, A.; Takeuchi, K.; Hayashi, T.; Tanioka, A.; Araki, T.; Tejima, S.; Noguchi, T.; Terrones, M.; Endo, M., High-performance multi-functional reverse osmosis membranes obtained by carbon nanotube·polyamide nanocomposite. *Sci. Rep.* **2015,** *5*, 13562.